Published in final edited form as:
Sci Transl Med. 2012 September 5; 4(150): 150ra122. doi:10.1126/scitranslmed.3004291.

Sleep-wake cycle and diurnal fluctuation of amyloid-β as biomarkers of brain amyloid pathology

Jee Hoon Roh[1,2,3], **Yafei Huang**[1], **Adam W. Bero**[1,2,3], **Tom Kasten**[1], **Floy R. Stewart**[1,2,3], **Randall J. Bateman**[1,2,3], and **David M. Holtzman**[1,2,3,4,*]

[1]Department of Neurology, Washington University School of Medicine, St. Louis, MO, 63110, USA

[2]Hope Center for Neurological Disorders, Washington University School of Medicine, St. Louis, MO, 63110, USA

[3]Charles F. and Joanne Knight Alzheimer's Disease Research Center, Washington University School of Medicine, St. Louis, MO, 63110, USA

[4]Department of Developmental Biology, Washington University School of Medicine, St. Louis, MO, 63110, USA

Abstract

Aggregation of amyloid-β (Aβ) in the brain begins to occur years prior to the clinical onset of Alzheimer's disease (AD). Prior to Aβ aggregation, levels of extracellular, soluble interstitial fluid (ISF) Aβ, which are regulated by neuronal activity and the sleep-wake cycle, correlate with the amount of Aβ deposition in the brain seen later. The amount and quality of sleep declines with aging and to a greater extent in AD. How sleep quality amount as well as the diurnal fluctuation in Aβ change with age and Aβ aggregation are not well understood. We report that a normal sleep-wake cycle and diurnal fluctuation of ISF Aβ is present in the brain of APPswe/PS1δE9 mice before Aβ plaque formation. Following plaque formation, the sleep-wake cycle markedly deteriorated and diurnal fluctuation of ISF Aβ dissipated. As in mice, diurnal fluctuation of cerebrospinal fluid (CSF) Aβ in young adult humans with presenilin mutations was also markedly attenuated with Aβ plaque formation. Virtual elimination of Aβ deposits in the mouse brain by active immunization with Aβ42 normalized the sleep-wake cycle and the diurnal fluctuation of ISF Aβ. These data suggest that Aβ aggregation disrupts the sleep-wake cycle and diurnal fluctuation of Aβ. Sleep-wake behavior and diurnal fluctuation of Aβ in the central nervous system appear to be functional and biochemical markers respectively of Aβ-associated pathology that should be explored in humans diagnostically prior to and following symptom onset and in response to treatment.

[*]To whom correspondence should be addressed: **David M. Holtzman, M.D**., Andrew B. and Gretchen P. Jones Professor and Chair, Department of Neurology, Washington University School of Medicine, 660 S. Euclid Ave. Campus Box 8111, Saint Louis, MO 63110, Administrator phone: (314) 747-0644, Office phone: (314) 362-9872, Fax: (314)362-2244, holtzman@neuro.wustl.edu.

Author Contributions: J.H.R, A.W.B., R.J.B, and D.M.H. designed the study. J.H.R. performed steady-state microdialysis, Aβ ELISA, lactate assays, sleep-wake cycle experiments, and immunization studies. F.R.S. harvested brain tissue and performed HJ3.4 and X-34 staining. H.Y., T.K., and R.J.B. collected and analyzed human data. J.H.R. wrote and edited the manuscript with critical revision from D.M.H. and coauthors.

Competing interests: D.M.H. and R. J.B. are scientific advisors to C2N Diagnostics, and are co-inventors on U.S. patent 7,892,845 "Methods for measuring the metabolism of neurally derived biomolecules *in vivo.*'" Washington University with D.M.H. and R.J.B. as co-inventors has also submitted the U.S. non-provisional patent application "Methods for measuring the metabolism of CNS derived biomolecules *in vivo*" serial #12/267',974. D.M.H. is on the scientific advisory board of Pfizer. D.M.H., has consulted for Bristol Myers Squibb. All other authors declare no competing interests.

Introduction

Aggregation of the Aβ peptide in the extracellular space of the brain is one of the pathologic hallmarks of AD. Aβ is produced from amyloid precursor protein (APP) by sequential cleavage by β- and γ-secretase (1–3) and exists as a soluble, monomeric form throughout life (4). Monomeric Aβ begins to aggregate in the human brain ~10–15 years prior to when the clinical symptoms and signs of AD become appreciable, by which time a substantial amount of neuronal and synaptic loss in several brain regions is present (5, 6). In humans with Aβ aggregation in the brain who are clinically asymptomatic (preclinical AD), there is evidence of decreased functional connectivity in brain networks affected by amyloid deposition (7, 8). There may be other functional changes associated with Aβ aggregation during preclinical AD (9). Identification of such factors will be important to better assess functional impairment during this period of time as well as to assess response to novel disease modifying therapies.

APP transgenic mice that develop Aβ aggregation in the brain are neuropathological and functional models of preclinical AD in that they develop Aβ aggregation, inflammation, neuritic dystrophy as well as functional disconnection between brain areas but do not develop marked neurodegeneration including tauopathy (10–13). Therefore, understanding Aβ metabolism and functional deficits induced by Aβ aggregation in such mice may provide useful clues to aid in development of early diagnosis in humans as well as provide insights into functional abnormalities induced by Aβ aggregation prior to significant cognitive decline.

Interstitial fluid (ISF) Aβ concentration in APP transgenic mice is closely associated with brain synaptic and neuronal activity before Aβ plaque formation (14, 15) and is related to subsequent amyloid plaque formation and growth *in vivo* (16). We previously reported in young APPswe transgenic and wild-type mice without Aβ plaques in the brain that ISF Aβ increases during wakefulness and decreases during sleep (17), similar to the diurnal fluctuation of cerebrospinal fluid (CSF) Aβ observed in humans (17–19). However, whether the sleep-wake cycle and Aβ fluctuation becomes disrupted following Aβ aggregation in the brain is not clear. Further, the causal relationship between changes in the sleep-wake cycle and changes in Aβ metabolism are not understood. Herein, we characterized the amount and quality of sleep and the degree of diurnal Aβ fluctuation across two brain regions with different vulnerability to Aβ deposition before and after the onset of Aβ aggregation in a mouse model of β-amyloidosis. We also assessed CSF Aβ levels over 36 hours in humans carrying mutations that cause autosomal dominant forms of AD. Moreover, we examined whether preventing Aβ aggregation was sufficient to normalize the sleep-wake cycle and biochemical abnormalities in the mouse model.

Results

Changes in the sleep-wake cycle and Aβ diurnal fluctuation with Aβ deposition

APPswe/PS1δE9 mice (20) at 3 months of age, before Aβ deposition begins, displayed a diurnal fluctuation of ISF Aβ in the hippocampus and in the striatum (Fig. 1A, D, G, J) and a normal sleep-wake cycle (Fig. 2A) , similar to that seen in wild-type littermates (Fig. S1A–F). APPswe/PS1δE9 mice begin to deposit substantial amounts of Aβ plaques in the hippocampus by 6 months of age, while striatal deposition is not detectable until 9 months Fig. S2). At 6 months, diurnal fluctuation of ISF Aβ was disrupted in the hippocampus (Fig. 1B, E), but maintained in the striatum (Fig. 1H, K). There was also a trend for an increase in wakefulness and a decrease in sleep during the light phase (Fig. 2B, G–I) at 6 months. At 9 months, when Aβ plaques were increased to a greater extent in hippocampus and now present in striatum (Fig. S2E, F), loss in diurnal fluctuation of ISF Aβ was observed in both

brain regions (Fig. 1C, F, I, L). There was also a marked disruption of the sleep-wake cycle with significantly increased wakefulness and decreased rapid eye movement (REM) and non-REM (NREM) sleep (Fig. 2). Absolute levels of ISF Aβ were decreased in the hippocampus and remained unchanged in the striatum (Fig. 1M, N).

Attenuated diurnal fluctuation of CSF Aβ in human subjects with Presenilin (PS) mutations

In addition to a loss of diurnal fluctuation of ISF Aβ seen in APPswe/PS1δE9 mice, we also observed attenuation of the diurnal pattern of Aβ in the CSF of humans with *PS* mutations who also had Aβ deposition as detected by amyloid imaging with Pittsburgh Compound B (PiB) (Fig. 3). Cosinor analysis was used to assess the diurnal patterns of CSF Aβ dynamics in mutation+, PiB−; mutation+, PiB+; and age-matched mutation- groups using mean-adjusted group average data after linear trend subtraction (19). Significant cosinor patterns were found in both mutation-and the mutation+, PiB− groups ($p<0.05$), but not in the mutation+, PiB+ group ($p>0.05$)(Fig. 3). Results from mutation carriers who are PiB− showed an attenuation of diurnal fluctuation of CSF Aβ42 in which the degree of attenuation is in between that seen in non-carriers and carriers who are PiB+ (Fig. 3A–C).

Normalization of sleep-wake cycle and Aβ diurnal fluctuation by active immunization

To investigate whether Aβ aggregation is responsible for the changes in sleep amount and quality as well as the attenuation of the diurnal fluctuation of ISF Aβ, we actively immunized APPswe/PS1δE9 mice starting at 1.5 months of age and then monthly with subcutaneous injections of synthetic $Aβ_{1–42}$ or phosphate buffered saline (PBS) and compared the patterns of ISF Aβ and the sleep-wake cycle at 9 months. PBS-treated APPswe/PS1δE9 mice showed a pattern of Aβ plaque deposition similar to untreated 9 month old APPswe/PS1δE9 mice (Fig. 4A, B). Diurnal fluctuation of ISF Aβ was absent in the hippocampus of PBS-treated animals and the mice had strongly disrupted sleep-wake patterns (Fig. 5A, B, D, E). In contrast, APPswe/PS1δE9 mice actively immunized with $Aβ_{1–42}$ showed markedly decreased Aβ deposits in the brain (Fig. 4C, D) and exhibited both a normal sleep-wake cycle and diurnal fluctuation of ISF Aβ at 9 months (Fig. 5G–L). During the light period, PBS-treated mice were awake 29.6 +/− 4.1 minutes per hour whereas Aβ42-vaccinated mice were awake 17.2 +/− 2.4 minutes per hour ($P=0.0256$) (Fig 5 A, D, G, J). Wild-type littermates had a normal sleep-wake cycle and diurnal fluctuation of endogenous Aβ through 9 months of age (Fig. S1G–L).

Changes in neuronal activity and the sleep-wake cycle following Aβ accumulation

Lactate is a marker of neuronal activity both *in vitro* and *in vivo* that it is increased during wakefulness and decreased during sleep (15, 21, 22). We measured ISF lactate in the hippocampus and striatum of APPswe/PS1δE9 mice and found differences across the dark- and light-phases. To investigate whether levels of lactate could be a biological marker of wakefulness irrespective of Aβ pathology in the brain, we compared the levels of ISF lactate and wakefulness in APPswe/PS1δE9 mice at different ages. Levels of ISF lactate showed a significant correlation with the amount of wakefulness at 3, 6, and 9 months (Fig. S3). Additional analysis of the amplitude of diurnal fluctuation of lactate as assessed by Cosinor analysis (23) showed a decrease in amplitude by 9 months of age (Fig. 6) corresponding to an increase in wakefulness. To further investigate a potential causal relationship between changes in Aβ metabolism and changes in brain neuronal activity, we compared the chronological changes in correlation between ISF Aβ and ISF lactate in relation to Aβ accumulation. Hippocampal levels of ISF lactate and ISF Aβ correlated at 3 and 6 months, but the correlation was lost by 9 months (Fig. S4A–C). This was validated in PBS-treated APPswe/PS1δE9 mice where there was no correlation between ISF lactate and ISF Aβ at 9 months (Fig. S5A). In contrast, APPswe/PS1δE9 mice actively immunized with $Aβ_{1–42,}$ maintained a significant correlation between levels of ISF lactate and ISF Aβ in the

hippocampus and striatum at 9 months Fig. S5B, D. These data demonstrate a strong relationship between the sleep-wake state and neuronal activity even after the acquisition of Aβ pathology and suggest the cause of ISF Aβ fluctuation disruption is more likely due to the biochemical effect of the formation of Aβ plaques resulting in sequestration of ISF Aβ and not due to a change in neuronal activity associated with sleep-wake cycle.

Loss of Aβ diurnal fluctuation associated with absolute decrease in ISF and CSF Aβ42

We also investigated whether ISF $A\beta_{42}$ behaved similarly to $A\beta_{1\text{-}x}$ and $A\beta_{x\text{-}40}$ in both hippocampus and striatum. At 3 months, ISF $A\beta_{x\text{-}42}$ showed diurnal fluctuation which was lost by 9 months in APPswe/PS1δE9 mice (Fig. S6). PBS-treated mice showed loss of diurnal fluctuation at 9 months similar to that seen in 9 month old untreated APPswe/PS1δE9 mice (Fig. S7A, C, E, G). In contrast, APPswe/PS1δE9 mice actively immunized with $A\beta_{1\text{–}42}$ had normal diurnal fluctuation of ISF $A\beta_{x\text{-}42}$ (Fig. S7B, D, F, H) and a marked decrease of amyloid plaques in the brain (Fig. S8). Also notable was that the absolute amount of ISF Aβ42 decreased between 3 and 9 months in the hippocampus in APPswe/PS1δE9 mice (Fig. 7A). In contrast to Aβ, levels of ISF lactate which does not aggregate in the brain continue fluctuating at 6 months with no change in absolute levels through nine months of age (Fig. 7B, E). Absolute levels of CSF Aβ42 in humans also decreased in those with Aβ plaque formation. The levels of CSF Aβ42 was highest in non-mutation carriers and lowest in PiB+ mutation carriers and the amount of CSF Aβ 42 inversely correlated with the amount of fibrillar Aβ in the brain as measured by amyloid imaging (Fig 7C, F).

Discussion

Herein, we found an Aβ accumulation-associated disruption of the sleep-wake cycle and loss of diurnal fluctuation of ISF Aβ in a mouse model of AD amyloidosis. Similar findings, namely loss of diurnal fluctuation of CSF Aβ associated with amyloid deposition, were also seen in humans with mutations that cause autosomal dominant AD. These changes were not seen in age-matched wild-type mice in ISF nor in age-matched humans lacking *PS* mutations in CSF, suggesting that over-expression of APP/PS1 transgenes associated with autosomal dominant AD in mice or some form of Aβ aggregation was responsible. The finding that active immunization with Aβ42 prevented the changes in sleep disruption as well as diurnal fluctuation of Aβ in mice and that aged littermates maintained both sleep-wake cycle and diurnal fluctuation of Aβ strongly suggest that Aβ accumulation rather than over-expression of transgenes is responsible for these changes.

The sleep-wake cycle is a fundamental property of the brain. Diurnal fluctuation of Aβ is a physiologic finding observed in brains of mice and humans that occurs prior to the development of Aβ plaque deposition. We found that the diurnal fluctuation of ISF Aβ was disrupted sequentially in line with a hierarchical deposition of Aβ plaques in different brain regions. As changes in Aβ fluctuation occurred prior to the changes in sleep quality and perturbation of neuronal activity, the results suggest that the changes in ISF Aβ fluctuation are likely due to a biochemical change in Aβ metabolism induced by plaque formation and not by changes in the sleep-wake cycle itself. Using mouse models of β-amyloidosis, we previously showed that sleep deprivation and administration of the neuropeptide orexin, which regulates arousal and wakefulness, acutely increased ISF Aβ and chronic sleep deprivation strongly increased Aβ plaque formation (17). Blocking orexin receptors acutely and chronically decreased ISF Aβ and plaque formation (17). These results suggested the possibility that sleep disruption and disorders might be a risk factor for development of Aβ deposition and possibly AD. Emerging evidence in humans suggests this may be the case (24, 25) though additional longitudinal studies with biomarkers are required since studies with elderly participants could not assess a cause/effect relationship between AD pathology and changes in sleep. While disrupted sleep has the potential to lead to Aβ aggregation, our

current results suggest that once Aβ aggregates, some of the damage it induces in the CNS leads to dysregulation of the sleep-wake cycle. Previous reports on AD patients and mouse models of Aβ amyloidosis support the possibility that the presence of Aβ-related pathology in the brain is associated with a disrupted sleep-wake cycle or circadian rhythm by affecting molecules including orexin, melatonin, and associated brain regions (26–32). Thus, there could be a positive feedback loop between the sleep-wake cycle and Aβ metabolism. The early increase in wakefulness possibly initiated by the aggregation of Aβ may accelerate Aβ accumulation which may lead to further neuronal dysregulation and increase sleep-wake cycle abnormalities.

Observations from this study also demonstrate that the sleep changes are likely due to Aβ aggregation and not the effect of aging. Recent human studies assessing CSF noted diurnal fluctuation of CSF Aβ in young adults was attenuated in older adults who were a mean age of 73.4 years. Whether this attenuation was due to aging or Aβ aggregation was not clear (19). The oldest APPswe/PS1δE9 mice used in this study only reached the equivalent of middle age and wild type littermates at the same age did not have sleep-associated impairments. As the mouse model we are using expresses mutations found in humans with dominantly inherited AD who begin to have AD pathology as young adults, we further investigated presymptomatic individuals within autosomal dominant AD families. In those young subjects (mean age of 42.4) with and without Aβ pathology in the brain, we demonstrated that the aggregation of Aβ in the brain is associated with the attenuation of diurnal fluctuation of Aβ in human CSF. This attenuation was not present in age-matched siblings that lacked these mutations. This suggests that changes in brain Aβ metabolism associated with amyloid plaque formation induces attenuation in the fluctuation of CSF Aβ independent of an effect of aging. While the change in diurnal fluctuation in CSF Aβ in presenilin carriers with vs. without amyloid deposition is significant, it is small suggesting it may be difficult to be used as a biomarker. However, if the changes in sleep quality and amount seen in APPswe/PS1δE9 mice are also present in humans, this may provide a very useful quantitative and functional endophenotype during the period of preclinical AD that can be assessed in response to therapeutic intervention.

Aβ aggregation was also associated with disruption of homeostatic fluctuation of neuronal activity in the brain. Before Aβ plaque deposition, there was a strong correlation between levels of ISF Aβ and ISF lactate, suggesting neuronal activity associated release of Aβ within the brain (14, 15, 33). The correlation between ISF Aβ and ISF lactate, however, was lost after substantial accumulation of Aβ in the brain. Sequential loss of correlation between ISF lactate and ISF Aβ with a decrease in absolute amount of ISF Aβ indicates that changes in the equilibrium between ISF Aβ and Aβ plaques may cause dissociation between ISF Aβ levels and neuronal activity. The decrease in absolute levels of ISF Aβ and CSF Aβ in humans with Aβ plaque formation suggests that soluble ISF and CSF Aβ is being sequestered by amyloid plaques consistent with other studies (4, 34). On the other hand, lactate, which does not aggregate within brain, did not show changes in absolute levels in ISF. The significant decrease in the fluctuation of lactate in both hippocampus and striatum by 9 months of age in APPswe/PS1δE9 mice occurred in concert with the changes in the sleep-wake cycle, the most prominent change of which was a marked increase in wakefulness during the light phase by 50%, a time when the animals would otherwise be sleeping the majority of the time. This increase in wakefulness may be very damaging to the brain in an additive fashion to other Aβ-linked pathways of damage as many studies have shown the important function of sleep to learning, memory, synaptic plasticity, and risk for other medical disorders (35–38). It is possible that the Aβ-induced changes to sleep are due to local cortical and hippocampal Aβ induced changes to synaptic activity and excitability occurring throughout affected brain regions (39–41). Of note, at all ages assessed in our studies, APPswe/PS1δE9 mice had no phenotypic or electroencephalogram (EEG) evidence

of seizures. Thus, the disruption of the sleep-wake cycle which may be due to synaptic alterations was not secondary to seizures.

Sleep-wake patterns of the human subjects who participated in this study were not investigated. Sleep changes in young adults with autosomal dominant AD before or after Aβ pathology in the brain will be important in future studies to determine whether similar changes in the sleep-wake cycle are present as Aβ pathology develops in the preclinical stages of disease. Since changes in the sleep-wake cycle and Aβ fluctuation in both mice and humans were all in the presence of presenilin mutations, it will be important in the future to assess whether the same changes occur in the absence of such mutations. Thus, it will also be interesting to determine if changes in the sleep-wake cycle are present in the preclinical stages of late-onset AD which would have very important implications both diagnostically as well as for therapeutic assessment.

Materials and methods

Mice

All studies were approved by the Animal Studies Committee at Washington University. Female APPswe/PS1δE9 on a B6C3 background (The Jackson Laboratory) mice (20) and their wild-type littermates (B6C3) were utilized at 3, 6, and 9 months of age for sleep-wake analysis and for microdialysis for ISF Aβ and lactate measurement. Aβ immunohistochemistry and X-34 staining were performed at the completion of experiments. Animals were given *ad libitum* access to food and water.

In vivo microdialysis

In vivo microdialysis to assess Aβ and lactate in the brain ISF of awake, freely behaving mice was performed as described (4, 15). Briefly, guide cannulae (BR-style, BioAnalytical Systems) were stereotaxically implanted into hippocampus (bregma −3.1 mm, 2.5 mm lateral to midline, 1.2 mm below the dura at a 12° angle) and striatum (bregma + 0.5 mm, 2.5 mm lateral to midline, 1.6 mm below the dura at a 14.5° angle), simultaneously. Probe placement in the regions of interest was confirmed by cresyl violet staining. Microdialysis probes (2 mm; 38 kDa molecular weight cut-off; BR-style, BioAnalytical Systems) were connected to a syringe pump (Stoelting Co.) and artificial cerebrospinal fluid (pH 7.35) containing (in mM) 1.3 Cl_2, 1.2 $MgSO_4$, 3 KCl, 0.4 KH_2PO_4, 25 $NaHCO_3$, and 122 NaC1 was continuously perfused through the microdialysis probe. For measurement of $A\beta_{1\text{-}x}$ and lactate in APPswe/PS1δE9 mice, a flow rate of 1.0 μl/min was utilized. For measurement of $A\beta_{x\text{-}40}$ in wild-type littermates and for measurement of $A\beta_{x\text{-}42}$ in APPswe/PS1δE9 and wild-type littermates a flow rate of 0.5 μl/min was used. Guide cannulae were implanted 2 weeks before the beginning of microdialysis. After insertion of microdialysis probe mice were habituated to a 12 hr light/dark cycle for 3 more days. On the 4^{th} day, samples were collected and stored for analyses.

Immunization

We actively immunized APPswe/PS1δE9 mice beginning at 1.5 months of age with synthetic $A\beta_{1–42}$ or phosphate buffered saline (PBS) as described (42). Briefly, $A\beta_{1–42}$ peptide was freshly prepared from lyophilized powder. Then, 2mg Aβ42 (human $A\beta_{1–42,}$ US Peptides) was added to 0.9 ml deionized water and the mixture was vortexed to generate a relatively uniform suspension. A l00μl aliquot of 10X PBS was added to make a final 1X PBS (0.15MNaCl, 0.01M sodium phosphate, pH 7.5). The suspension was vortexed again and incubated overnight at 37°C. Aβ42 was 1:1 (v/v) emulsified with complete Freund's adjuvant for the first immunization, followed by boost injections with incomplete Freund's adjuvant at 2, 4 weeks, and monthly thereafter until 9 months. For PBS treatment, the exact

same methods were used except using PBS instead of $A\beta_{1–42.}$ Titers were determined by serial dilutions of sera against Aβ42 protein which had been coated on ELISA plates. Detection used goat anti-mouse immunoglobulin conjugated to horseradish peroxidase and slow-TMB (3,3',5,5'-tetramethyl benzidine; Sigma-Aldrich) substrate. Titers were defined as the dilution yielding 50% of the maximal signal.

ELISA

Microdialysis samples were analyzed for $A\beta_{x\text{-}40,}$ $A\beta_{x\text{-}42,}$ or $A\beta_{1\text{-}x}$ using sandwich ELISAs. Briefly, $A\beta_{x\text{-}40,}$ $A\beta_{x\text{-}42,}$ and $A\beta_{1\text{-}x}$ were captured using monoclonal antibodies targeted against amino acids 35–40 (HJ2), 37–42 (HJ7.4) and 13–28 (m266) of Aβ, respectively. For $A\beta_{x}$. 40 and $A\beta_{x\text{-}42}$ assays, a biotinylated central domain monoclonal antibody (HJ5.1) followed by streptavidin-poly-HRP-40 (Fitzgerald) was used for detection. For $A\beta_{1\text{-}x}$ assays, a biotinylated N-terminal domain monoclonal antibody (3D6) followed by streptavidin-poly-HRP-20 (Fitzgerald) was used. The antibodies m266 and 3D6 were generous gifts from Eli Lilly. All assays were developed using Super Slow ELISA TMB (Sigma-Aldrich) and read on a Bio-Tek Synergy 2 plate reader at 650 nm.

Lactate assay

An enzymatic lactate assay kit (BioVision) was used to measure ISF lactate according to the manufacturer's instructions. Assays were read on a Bio-Tek Synergy 2 plate reader at 570 nm. To calculate the absolute values of steady-state concentration of lactate being dialyzed, the zero flow extrapolation method was used by varying flow rates from 0.4 to 1.2 μl/min (43). Zero flow data for each mouse were fit with an exponential decay regression and the maximum concentration at the point at which there is no flow of the perfusion buffer was calculated using GraphPad Prism 5.0 software, as described (44).

Sleep-wake monitoring

Polysomnographic sleep-wake cycle analysis of mice was performed as described previously (15, 17). Briefly, electroencephalograph (EEG) and electromyogram (EMG) electrodes were implanted simultaneously with the microdialysis guide cannula. For EEG recording, two stainless steel screws attached to wire electrodes were placed over the right frontal bone (bregma +1.0 mm, 1.5 mm lateral to midline) and the right parietal bone (bregma −3.0 mm, 2.5 mm lateral to midline). Two wire electrodes were directly inserted into the neck musculature for EMG recording. The ground electrode was placed on the skull over the cerebellum. Insulated leads from the EEG and EMG electrodes were soldered to a mini-connector. After surgery, mice were housed in 12 hour light/ 12 hour dark for 2 weeks before recording began. To monitor the sleep-wake cycle, mice were transferred to recording cages maintained in 12 hour light/ 12 hour dark conditions (light phase began at 6 a.m.) and the mini-connector was connected to flexible recording cables. Mice were habituated to the recording cages for 3 days. At the end of the habituation period, EEG and EMG recording began simultaneously with collection of microdialysis samples. EEG and EMG signals were displayed on a monitor and stored in a computer for analysis of sleep states. EEG and EMG recordings were assessed using a P511K A.C. Pre-amplifier (Grass-Telefactor Instruments), digitized with a DigiData 1440A Data Acquisition System (Molecular Devices), and recorded digitally using pClamp 10.2 (Molecular Devices). EEG and EMG signals were filtered (EEG: high pass 1 Hz; low pass 30 Hz; EMG: high pass 10 Hz; low pass 100 Hz) and used to identify vigilance states. EEG and EMG recordings were scored semi-automatically using sleep scoring software (SleepSign, Kissei Comtec Co., LTD., Japan) and binned into 10-sec epochs as wakefulness, rapid eye movement (REM) sleep, and non-REM (NREM) sleep on the basis of standard criteria of rodent sleep. Semi-automatic sleep scoring was visually inspected and corrected when appropriate. The

automatic analysis and visual inspection was performed in a blinded state to the genotype and age of mice.

Plaque deposition analyses

After mice were perfused with PBS transcardially, brains were removed, fixed in 4% paraformaldehyde for 24 hrs (4°C), cryoprotected with 30% sucrose in PBS (4°C), frozen in powdered dry ice, and cut on a freezing sliding microtome. Serial coronal sections (50 μm section thickness) were collected from the genu of the corpus callosum to caudal hippocampus. Sections (each separated by 300 μm) were stained with biotinylated HJ3.4 ($A\beta_{1–13}$) antibody to visualize Aβ immunopositive plaques or X-34 dye to visualize fibrillar amyloid plaques. Immunostained sections and X-34-stained sections were imaged using a NanoZoomer slide scanner (Hamamatsu Photonics). Quantitative analysis of percent area covered by immuno- or X-34-positive staining was performed as described previously (43). Briefly, images of immunostained sections were exported with NDP viewer software (Hamamatsu Photonics), converted to 8-bit grayscale using ImageJ software (National Institutes of Health), thresholded to highlight Aβ-specific staining and analyzed using ACDSee Pro 2 software (ACD Systems). Images of X-34-stained sections were converted to 16-bit grayscale, thresholded to highlight X-34-specific staining and analyzed using Image J software. A mouse brain atlas (45) was used to identify hippocampus (−1.7, −2.0, −2.3) and striatum (0.8, 0.5, 0.2) for quantitative analysis of immuno- and X-34-positive staining.

Human CSF analysis

Human participants were enrolled for the Familial Adult Children Study (FACS) conducted by the Knight Alzheimer Disease Research Center (ADRC) at Washington University. Mutations in *PS1* and *PS2* were genotyped for each participant at the ADRC Genetics Core. For participants with *PS* mutations, we determined the status of their brain amyloid deposition by PiB Positron Emission tomography (PET) scan. A mean cortical binding potential (MCBP) of 0.2 or greater was considered amyloid plaque positive (PiB+) (46). Serial CSF samples were collected from participants with mutations that are known to cause autosomal dominant AD and PiB− (mutation+PiB−, n=4), those with mutations and PiB+ (mutation+PiB+, n=4) and age matched no mutation carriers (mutation−, n=4). The samples were collected at the same time of day, starting at ~8AM for each participant. Samples were analyzed for concentrations of Aβ40 and Aβ42 using ELISA (19). The average ages for the mutation−, mutation+PiB−, and mutation+PiB+ group were 38.0±1.4, 46.3±16.9, and 43.0±10.3 years, respectively. Participants in mutation+ PiB− group had two types of PS1 mutations (His 163 Arg orPSl Ala 79 Val) and one type of PS2 mutation (Asn 141 Ile). Three types of PS1 mutation (PS1 Leu 226 Arg, His 163 Arg, or Met 146 Leu) and one type of PS2 mutation (Asn 141 Ile) were present in subjects in the mutation+PiB+ group. There was no statistical difference in age between groups (p=0.602). Circadian patterns of Aβ levels were investigated for the three groups using Cosinor analysis using the mean-adjusted group average data as described before (19). The mean value of CSF Aβ42 obtained over 36 hours was used for comparison of absolute values.

Statistical analysis

Statistical significance was determined by two-tailed Student’s t-test, if the data sets fulfilled the normality test (Kolmogorov-Smirnov test). When the data set did not meet the assumptions of a parametric test, Mann-Whitney Rank Sum Test was performed. One-way ANOVA followed by Tukey’s post hoc test for multiple comparisons was performed, if the data sets fulfilled the equal variance test (Levene’s test) and normality test (Kolmogorov-Smirnov test). If data sets did not fulfill both tests, Kruskal-Wallis test was performed. Pearson test was used for correlation analysis. Single cosinor analysis was used to analyze the 24-hour circadian patterns of ISF lactate fluctuation in each animal using Prism

(GraphPad Software) (19). A cosine transformation was applied to the time variable using 24 hours as the default circadian cycle and amplitude (distance between the peak and midline of the Aβ oscillation (mesor)) was calculated for each mouse (19, 23). In the human study, mean-adjusted group average data was used for analysis. Cosinor analysis was applied to data after linear trend was subtracted from the group-averaged Aβ values. All statistical analyses were performed using Prism version 4.0 for Windows (GraphPad Software) and SPSS 15.0 for Windows (SPSS Inc.). Values were accepted as significant if $P < 0.05$.

Supplementary Material

Refer to Web version on PubMed Central for supplementary material.

Acknowledgments

We thank Eli Lilly and Co. for generously providing m266 and biotinylated 3D6 anti-Aβ antibodies. We thank Jae-Eun Kang, Joseph M. Castellano, John R. Cirrito, Hong Jiang, and Mary Beth Finn for advice and discussions.

Funding: This work was supported by American Academy of Neurology Clinical Research Training Fellowship (J.H.R), P01AG026276-S1 (R.J.B.), K23AG03094604 (R.J.B.), R01NS065667 (R.J.B.), an Elison Medical Foundation Senior Scholar Award (D.M.H.), P01NS074969 (D.M.H.), AG13956 (D.M.H.), P30NS057105 (D.M.H.) and the Cure Alzheimer's Fund (D.M.H.).

REFERENCES

1. Selkoe DJ. Alzheimer's disease:genes proteins and therapy. Physiological reviews. 2001 Apr. 81:741. [PubMed: 11274343]
2. Golde TE, Eckman CB, Younkin SG. Biochemical detection of Abeta isoforms: implications for pathogenesis diagnosis and treatment of Alzheimer's disease. Biochimica et biophysica acta. 2000 Jul 26.1502:172. [PubMed: 10899442]
3. Haass C, Kaether C, Thinakaran G, Sisodia S. Trafficking and Proteolytic Processing of APP. Cold Spring Harbor perspectives in medicine. 2012 May.2:a006270. [PubMed: 22553493]
4. Cirrito JR, et al. In vivo assessment of brain interstitial fluid with microdialysis reveals plaque-associated changes in amyloid-beta metabolism and half-life. The Journal of neuroscience : the official journal of the Society for Neuroscience. 2003 Oct 1.23:8844. [PubMed: 14523085]
5. Holtzman DM, Morris JC, Goate AM. Alzheimer's disease: the challenge of the second century. Science translational medicine. 2011 Apr 6.3 77srl.
6. Sperling RA, et al. Toward defining the preclinical stages of Alzheimer's disease: recommendations from the National Institute on Aging-Alzheimer's Association workgroups on diagnostic guidelines for Alzheimer's disease. Alzheimer's & dementia : the journal of the Alzheimer's Association. 2011 May.7:280.
7. Sperling RA, et al. Amyloid deposition is associated with impaired default network function in older persons without dementia. Neuron. 2009 Jul 30.63:178. [PubMed: 19640477]
8. Sheline YI, et al. Amyloid plaques disrupt resting state default mode network connectivity in cognitively normal elderly. Biol Psychiatry. 2010 Mar 15.67:584. [PubMed: 19833321]
9. Holtzman DM, Goate A, Kelly J, Sperling R. Mapping the road forward in Alzheimer's disease. Science translational medicine. 2011 Dec 21.3 114ps48.
10. Jucker M. The benefits and limitations of animal models for translational research in neurodegenerative diseases. Nature medicine. 2010 Nov.16:1210.
11. Duyckaerts C, Potier MC, Delatour B. Alzheimer disease models and human neuropathology: similarities and differences. Acta neuropathologica. 2008 Jan.115:5. [PubMed: 18038275]
12. Gotz J, Ittner LM. Animal models of Alzheimer's disease and frontotemporal dementia. Nature reviews Neuroscience. 2008 Jul.9:532.

13. Bero AW, et al. Bidirectional Relationship between Functional Connectivity and Amyloid-beta Deposition in Mouse Brain. The Journal of neuroscience : the official journal of the Society for Neuroscience. 2012 Mar 28.32:4334. [PubMed: 22457485]
14. Cirrito JR, et al. Synaptic activity regulates interstitial fluid amyloid-beta levels in vivo. Neuron. 2005 Dec 22.48:913. [PubMed: 16364896]
15. Bero AW, et al. Neuronal activity regulates the regional vulnerability to amyloid-beta deposition. Nature neuroscience. 2011 Jun.14:750.
16. Yan P, et al. Characterizing the appearance and growth of amyloid plaques in APP/PS1 mice. The Journal of neuroscience : the official journal of the Society for Neuroscience. 2009 Aug 26.29:10706. [PubMed: 19710322]
17. Kang JE, et al. Amyloid-beta dynamics are regulated by orexin and the sleep-wake cycle. Science. 2009 Nov 13.326:1005. [PubMed: 19779148]
18. Bateman RJ, Wen G, Morris JC, Holtzman DM. Fluctuations of CSF amyloid-beta levels: implications for a diagnostic and therapeutic biomarker. Neurology. 2007 Feb 27.68:666. [PubMed: 17325273]
19. Huang Y, et al. Effects of age and amyloid deposition on Abeta dynamics in the human central nervous system. Archives of neurology. 2012 Jan.69:51. [PubMed: 21911660]
20. Savonenko A, et al. Episodic-like memory deficits in the APPswe/PSldE9 mouse model of Alzheimer's disease: relationships to beta-amyloid deposition and neurotransmitter abnormalities. Neurobiol Dis. 2005 Apr.18:602. [PubMed: 15755686]
21. Pellerin L, Magistretti PJ. Glutamate uptake into astrocytes stimulates aerobic glycolysis: a mechanism coupling neuronal activity to glucose utilization. Proceedings of the National Academy of Sciences of the United States of America. 1994 Oct 25.91:10625. [PubMed: 7938003]
22. Uehara T, Sumiyoshi T, Itoh H, Kurata K. Lactate production and neurotransmitters; evidence from microdialysis studies. Pharmacol Biochem Behav. 2008 Aug.90:273. [PubMed: 18502489]
23. Benavides A, Siches M, Llobera M. Circadian rhythms of lipoprotein lipase and hepatic lipase activities in intermediate metabolism of adult rat. Am J Physiol. 1998 Sep.275:R811. [PubMed: 9728079]
24. Yaffe K, et al. Sleep-disordered breathing, hypoxia, and risk of mild cognitive impairment and dementia in older women. JAMA. 2011 Aug 10.306:613. [PubMed: 21828324]
25. Tranah GJ, et al. Circadian activity rhythms and risk of incident dementia and mild cognitive impairment in older women. Annals of neurology. 2011; 70:722. [PubMed: 22162057]
26. Volicer L, Harper DG, Manning BC, Goldstein R, Satlin A. Sundowning and circadian rhythms in Alzheimer's disease. Am J Psychiatry. 2001 May.158:704. [PubMed: 11329390]
27. Vitiello MV, Borson S. Sleep disturbances in patients with Alzheimer's disease: epidemiology, pathophysiology and treatment. CNS Drugs. 2001; 15:777. [PubMed: 11602004]
28. Fronczek R, et al. Hypocretin (orexin) loss in Alzheimer's disease. Neurobiol Aging. 2011 May 3.
29. Wu YH, Swaab DF. Disturbance and strategies for reactivation of the circadian rhythm system in aging and Alzheimer's disease. Sleep Med. 2007 Sep.8:623. [PubMed: 17383938]
30. Wu YH, Swaab DF. The human pineal gland and melatonin in aging and Alzheimer's disease. J Pineal Res. 2005 Apr.38:145. [PubMed: 15725334]
31. Zhang B, et al. Impaired rapid eye movement sleep in the Tg2576 APP murine model of Alzheimer's disease with injury to pedunculopontine cholinergic neurons. Am J Pathol. 2005 Nov. 167:1361. [PubMed: 16251420]
32. Jyoti A, Plano A, Riedel G, Platt B. EEG, activity, and sleep architecture in a transgenic AbetaPPswe/PSENlA246E Alzheimer's disease mouse. J Alzheimer s Dis. 2010; 22:873.
33. Kamenetz F, et al. APP processing and synaptic function. Neuron. 2003 Mar 27.37:925. [PubMed: 12670422]
34. Hong S, et al. Dynamic analysis of amyloid beta-protein in behaving mice reveals opposing changes in ISF versus parenchymal Abeta during age-related plaque formation. The Journal of neuroscience : the official journal of the Society for Neuroscience. 2011 Nov 2.31:15861. [PubMed: 22049429]

35. Diekelmann S, Born J. The memory function of sleep. Nature reviews Neuroscience. 2010 Feb. 11:114.
36. Donlea JM, Thimgan MS, Suzuki Y, Gottschalk L, Shaw PJ. Inducing sleep by remote control facilitates memory consolidation in Drosophila. Science. 2011 Jun 24.332:1571. [PubMed: 21700877]
37. Maret S, Faraguna U, Nelson AB, Cirelli C, Tononi G. Sleep and waking modulate spine turnover in the adolescent mouse cortex. Nature neuroscience. 2011 Nov.14:1418.
38. Pack AI, Pien GW. Annual review of medicine. 2011; 62:447.
39. Kuchibhotla KV, Lattarulo CR, Hyman BT, Bacskai BJ. Synchronous hyperactivity and intercellular calcium waves in astrocytes in Alzheimer mice. Science. 2009 Feb 27.323:1211. [PubMed: 19251629]
40. Vyazovskiy VV, et al. Local sleep in awake rats. Nature. 2011 Apr 28.472:443. [PubMed: 21525926]
41. Busche MA, et al. Clusters of hyperactive neurons near amyloid plaques in a mouse model of Alzheimer's disease. Science. 2008 Sep 19.321:1686. [PubMed: 18802001]
42. Schenk D, et al. Immunization with amyloid-beta attenuates Alzheimer-disease-like pathology in the PDAPP mouse. Nature. 1999 Jul 8.400:173. [PubMed: 10408445]
43. Kim J, et al. Overexpression of low-density lipoprotein receptor in the brain markedly inhibits amyloid deposition and increases extracellular A beta clearance. Neuron. 2009 Dec 10.64:632. [PubMed: 20005821]
44. Menacherry S, Hubert W, Justice JB Jr. In vivo calibration of microdialysis probes for exogenous compounds. Anal Chem. 1992 Mar 15.64:577. [PubMed: 1580357]
45. Franklin, KB.; Paxinos, G. The Mouse Brain in Stereotaxic Coordinates. ed. 1st. San Diego: Academic Press; 1996. p. 216
46. Fagan AM, et al. Cerebrospinal fluid tau and ptau(181) increase with cortical amyloid deposition in cognitively normal individuals: implications for future clinical trials of Alzheimer's disease. EMBO molecular medicine. 2009 Nov.1:371. [PubMed: 20049742]

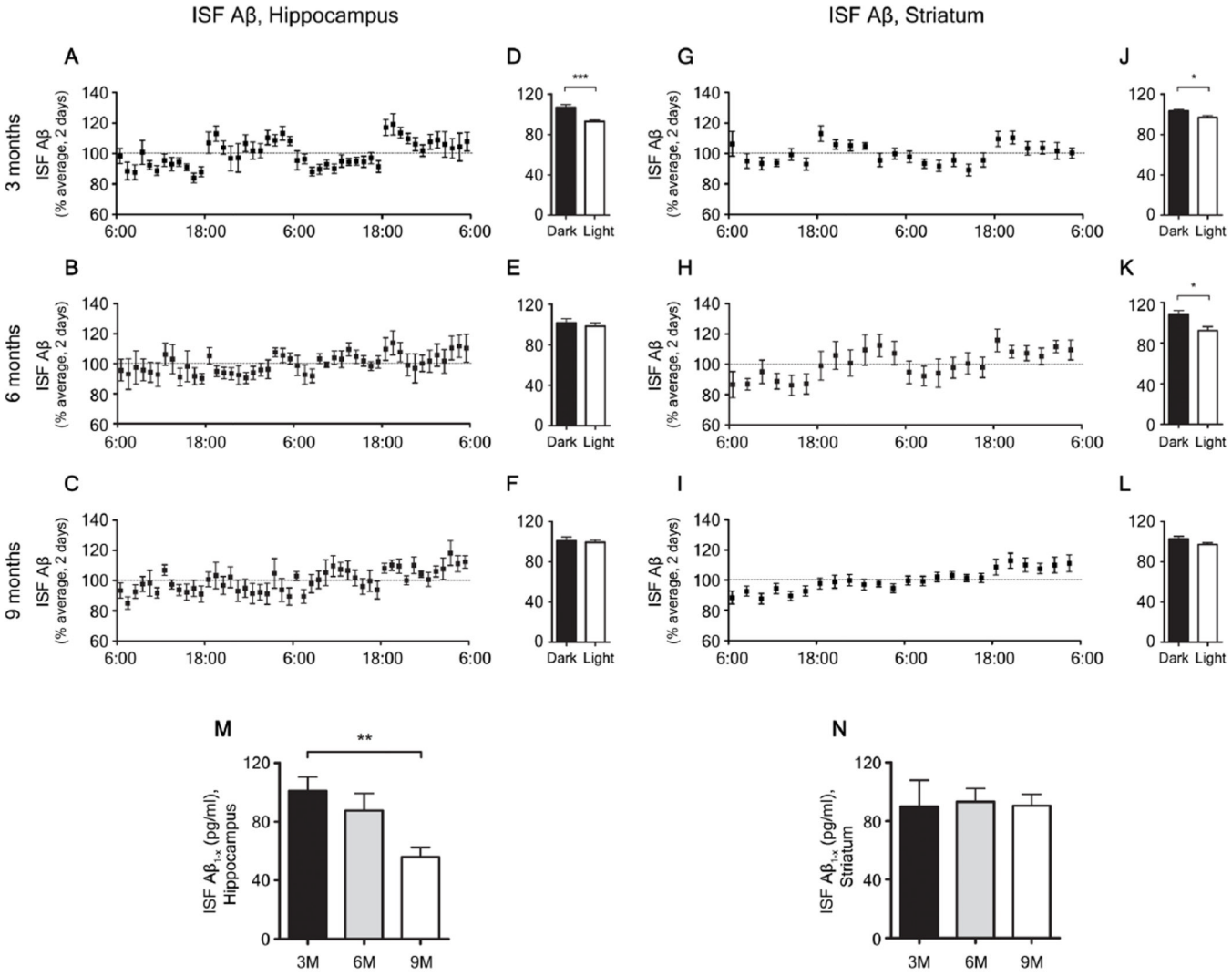

Figure 1.

Chronological changes in sleep-wake patterns and diurnal fluctuations of interstitial fluid (ISF) amyloid beta (Aβ) in APPswe/PS1δE9 mice. **(A–C, G–I)** Diurnal changes of ISF $Aβ_{1-x}$ in APPswe/PS1δE9 mice at 3, 6, 9 months across 2 days shown as % average of 2 days of absolute values of ISF $Aβ_{1-x}$ in the hippocampus **(A–C)** and striatum **(G–I)**. **(D–F, J–L)** Comparison of % average of 2 days of ISF $Aβ_{1-x}$ between dark and light periods in the hippocampus **(D–F)** and striatum **(J–L)** of each age group (n = 6–8 per group; two tailed t-test). **(M, N)** Absolute levels of ISF $Aβ_{1-x}$ in the hippocampus **(M)** and striatum **(N)** of 3, 6, and 9 month old APPswe/PS1δE9 mice (n = 6–8 per group; one-way ANOVA, followed by Tukey's *post hoc* test). $^{*}P < 0.05$; $^{**}P < 0.01$; $^{***}P < 0.001$. Values represent mean ± s.e.m.

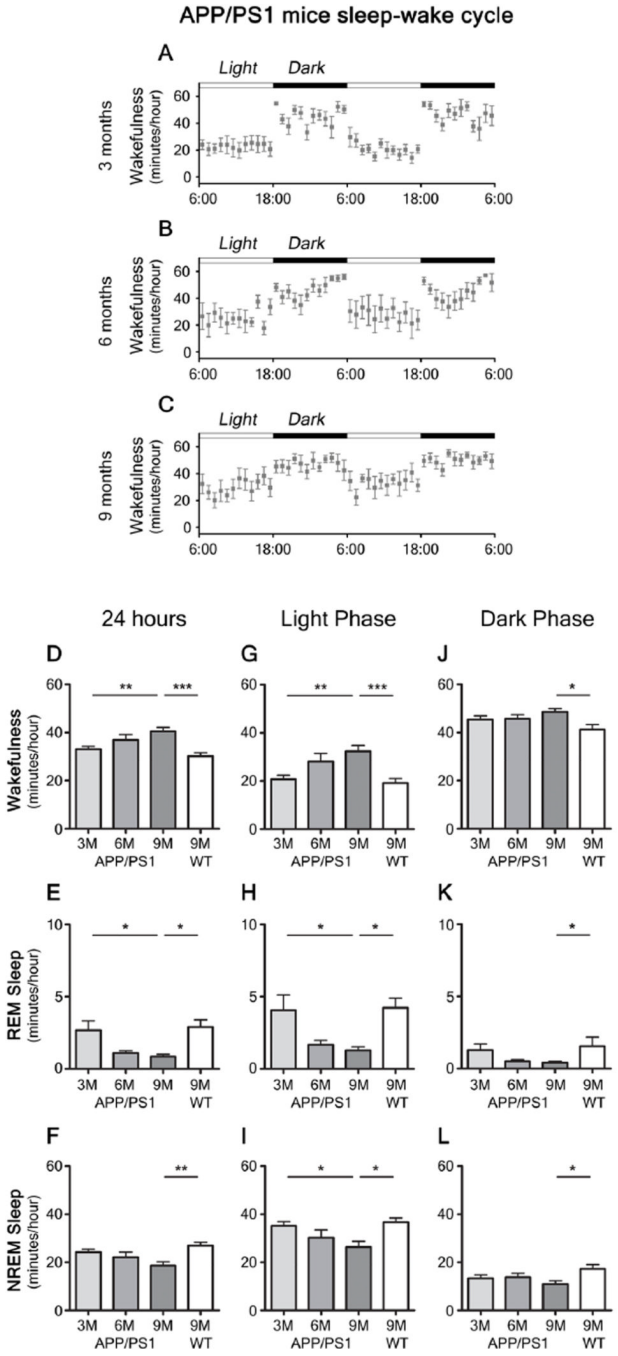

Figure 2.

Sleep-wake patterns in 3, 6, and 9 month old APPswe/PS1δE9 mice. **(A–C)** Sleep-wake patterns in 3, 6, and 9 month old APPswe/PS1δE9 mice across 2 days (2 light-dark periods) assessed as minutes awake per hour. **(D–L)** Chronological changes of minutes per hour spent in wakefulness, rapid eye movement (REM) sleep, and non-REM (NREM) sleep in 3, 6, and 9 month old APPswe/PS1δE9 mice and 9 month old wild-type littermates (B6C3). Analysis of a whole 24 hour period **(D–F)**, analysis during light period **(G–I)**, and analysis during dark period **(J–L)** (n = 6–8 per group; one-way ANOVA, Tukey's *post hoc* test for multiple comparisons). $*P < 0.05$; $**P < 0.01$; $***p < 0.001$. Values represent mean ± s.e.m.

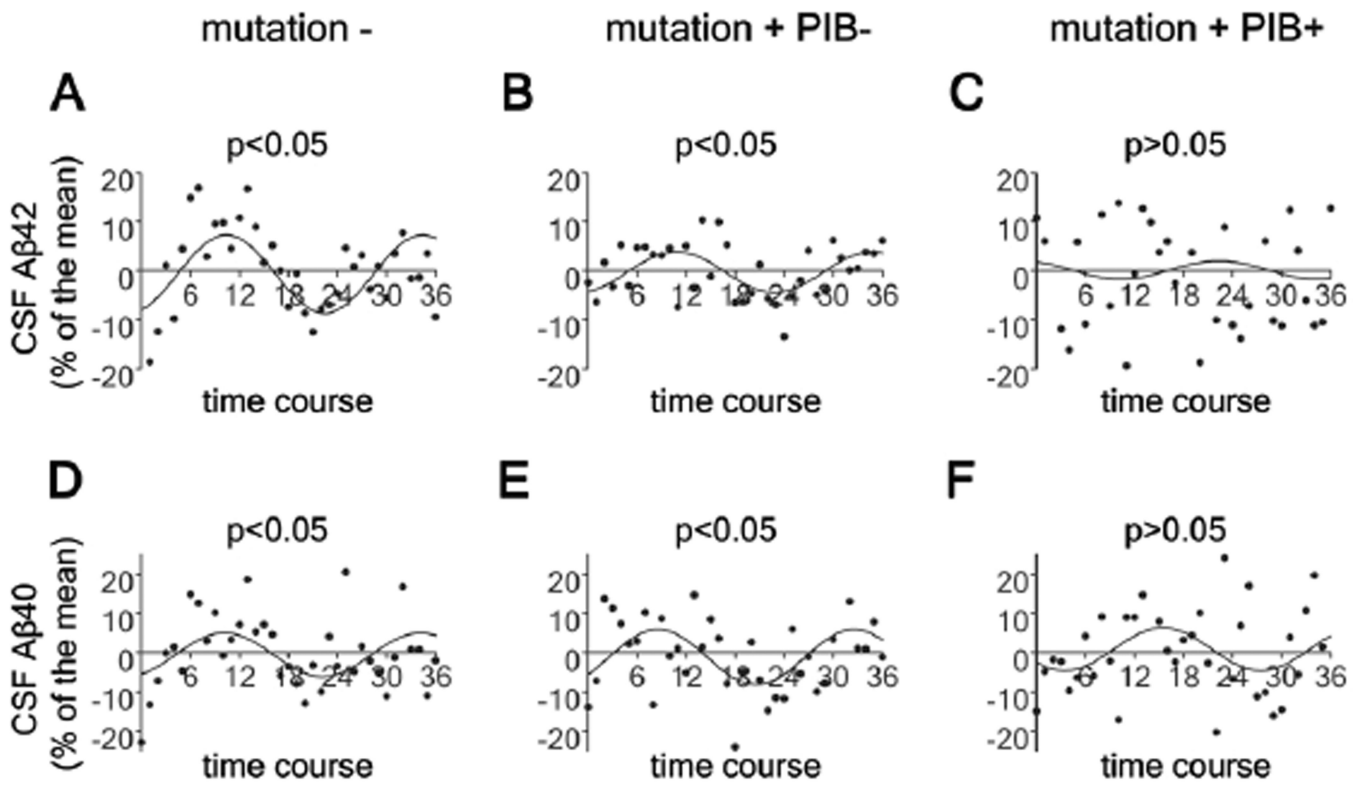

Figure 3.

Attenuated diurnal fluctuation of CSF Aβ in mutation carriers in autosomal dominant Alzheimer's disease (AD) families. **(A–F)** Diurnal fluctuation of CSF ISF Aβ40 and Aβ42 across 36 hours in no mutation carriers (mutation−; N=4) **(A, D)**, mutation carriers who are PiB−(mutation+PiB−; N=4) **(B, E)** and mutation carriers who are PiB+ (mutation+PiB+; N=4) **(C, F)** as shown by cosinor curves. Cosinor analysis was used to assess diurnal patterns of CSF Aβ dynamics in each group and diurnal patterns were considered significant when amplitudes were different from zero ($P < 0.05$).

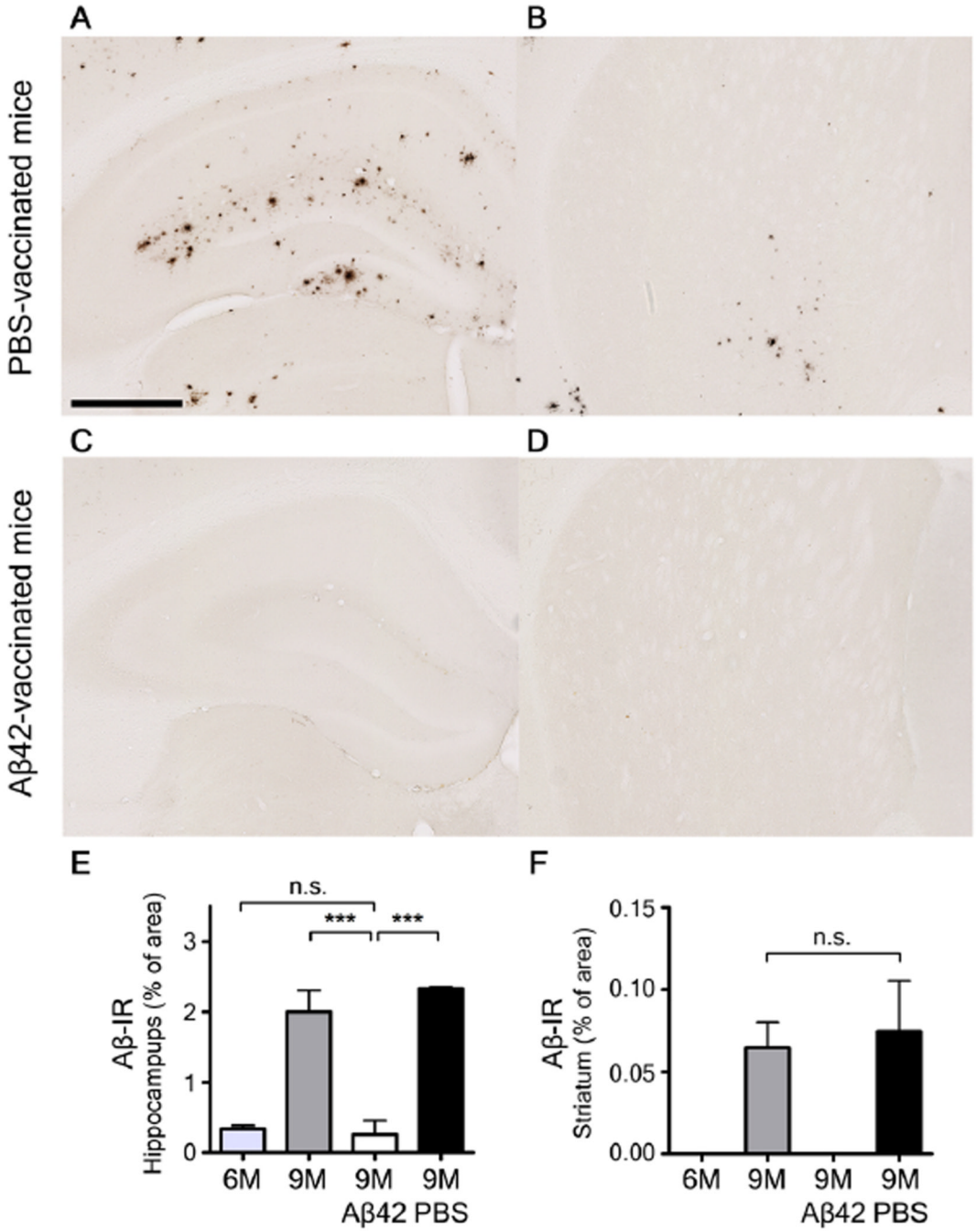

Figure 4.

Aβ plaque deposition in the hippocampus and striatum in 9 month old phosphate buffered saline (PBS)-treated and $A\beta_{42}$-immunized APPswe/PS1δE9 mice. **(A–D)** Representative brain sections of the hippocampus **(A, C)** and striatum **(B, D)** of mice from each group stained with HJ 3.4 antibody to visualize Aβ immunoreactive plaques (Aβ-IR). **(E, F)** Amount of Aβ deposition in the PBS-treated mice and $A\beta_{42}$-vaccinated mice are shown with amount of Aβ deposition in six and nine month old APPswe/PS1δE9 mice in the hippocampus **(E)** and striatum **(F)** (n=5–6 in each group; two tailed t-test). ***$P < 0.001$. n.s.

stands for not statistically significant. Values represent mean ± s.e.m. Scale bar in **(A)** represents 500μm.

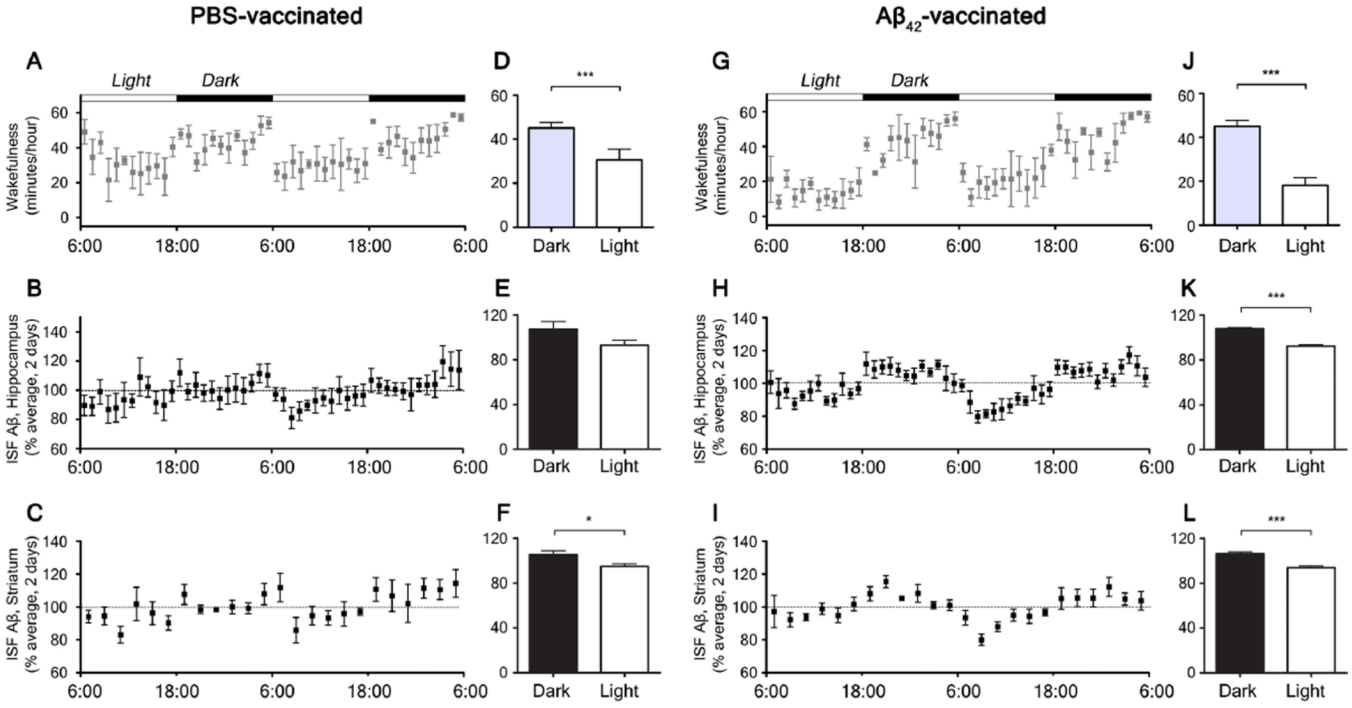

Figure 5.

Sleep-wake patterns and diurnal fluctuation of interstitial fluid (ISF) Aβ in 9 month old phosphate buffered saline (PBS)-treated and $A\beta_{42}$-immunized APPswe/PS1δE9 mice. **(A, G)** Sleep-wake patterns in 9 month old PBS-treated **(A)** and $A\beta_{42}$-immunized **(G)** APPswe/PS1δE9 mice across 2 days (2 light-dark periods) shown as minutes awake per hour. **(D, J)** Comparison of minutes awake per hour between the dark and light periods in each group (n = 5–6 per group; two tailed t-test). **(B, H)** Diurnal fluctuation of ISF $A\beta_{1-x}$ in the hippocampus of 9 month old PBS-treated **(B)** and Aβ42-immunized **(H)** APPswe/PS1δE9 mice across 2 days presented as % average of absolute values of ISF $A\beta_{1-x}$**(E, K)** Comparison of % average of absolute values of ISF $A\beta_{1-x}$ in the hippocampus between the dark and light periods (n = 5–6 per group; two tailed t-test). **(C, I)** Diurnal fluctuation of ISF $A\beta_{1-x}$ in the striatum of 9 month old PBS-vaccinated **(C)** and $A\beta_{42}$-vaccinated **(I)** APPswe/PS1δE9 mice across 2 days. **(F, L)** Comparison of % average of absolute values of ISF $A\beta_{1-x}$ in the striatum between the dark and light periods (n = 5–6 per group; two tailed t-test). $^{*}P < 0.05$; $^{***}p < 0.001$. Values represent mean ± s.e.m.

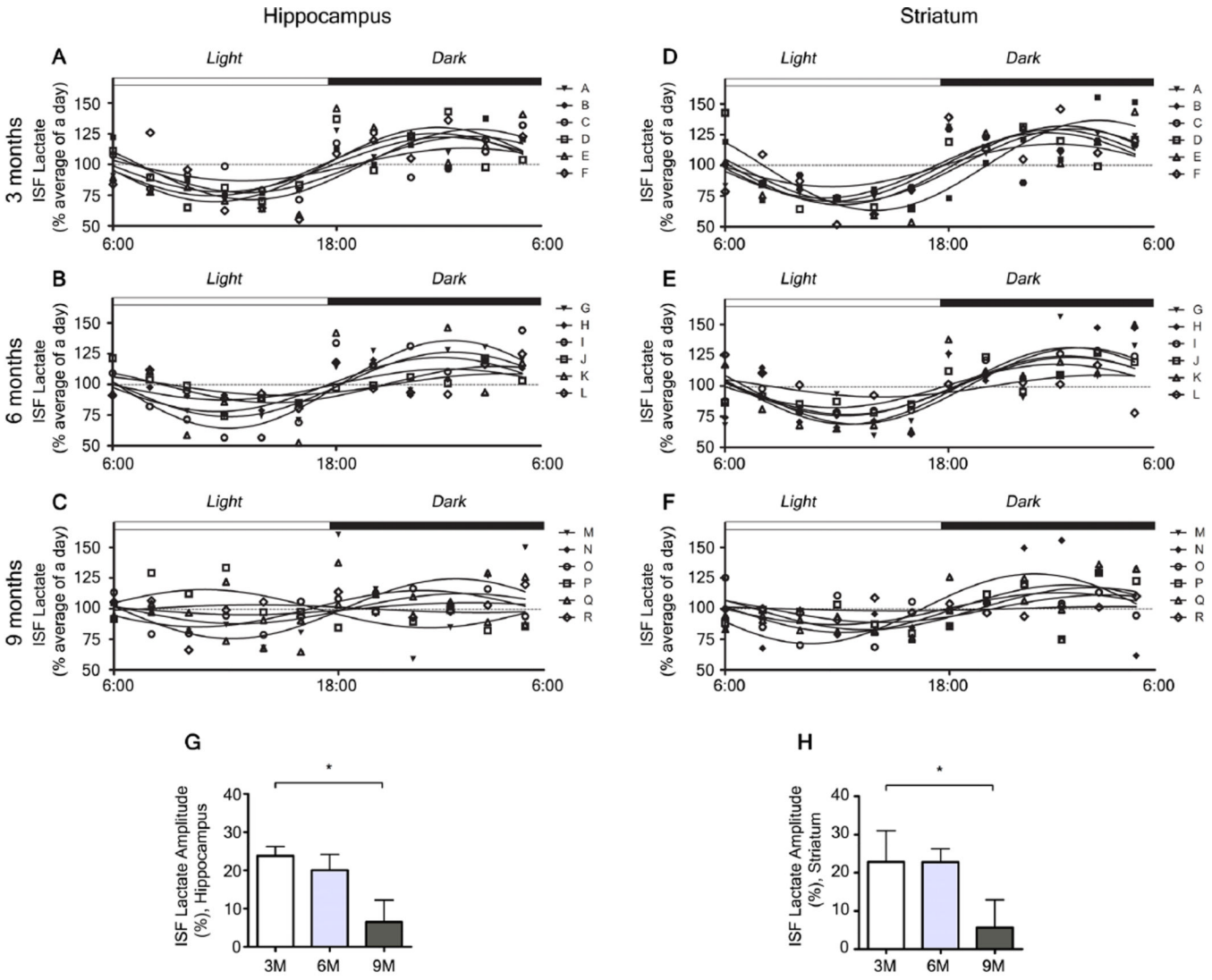

Figure 6.

Chronological changes in the amplitude of diurnal fluctuation of interstitial fluid (ISF) lactate in 3, 6, and 9 month old APPswe/PS1δE9 mice. **(A–F)** Diurnal fluctuation of ISF lactate in the hippocampus **(A–C)** and in the striatum **(D–F). (G, H)** Chronological changes in the amplitude of diurnal fluctuation in the hippocampus **(G)** and in the striatum **(H)** as measured by amplitude of cosinor analysis (n = 6 per group; one-way ANOVA after cosinor analysis for measurement of amplitude, Tukey's *post hoc* test for multiple comparisons). *$P < 0.05$. Values represent mean ± s.e.m.

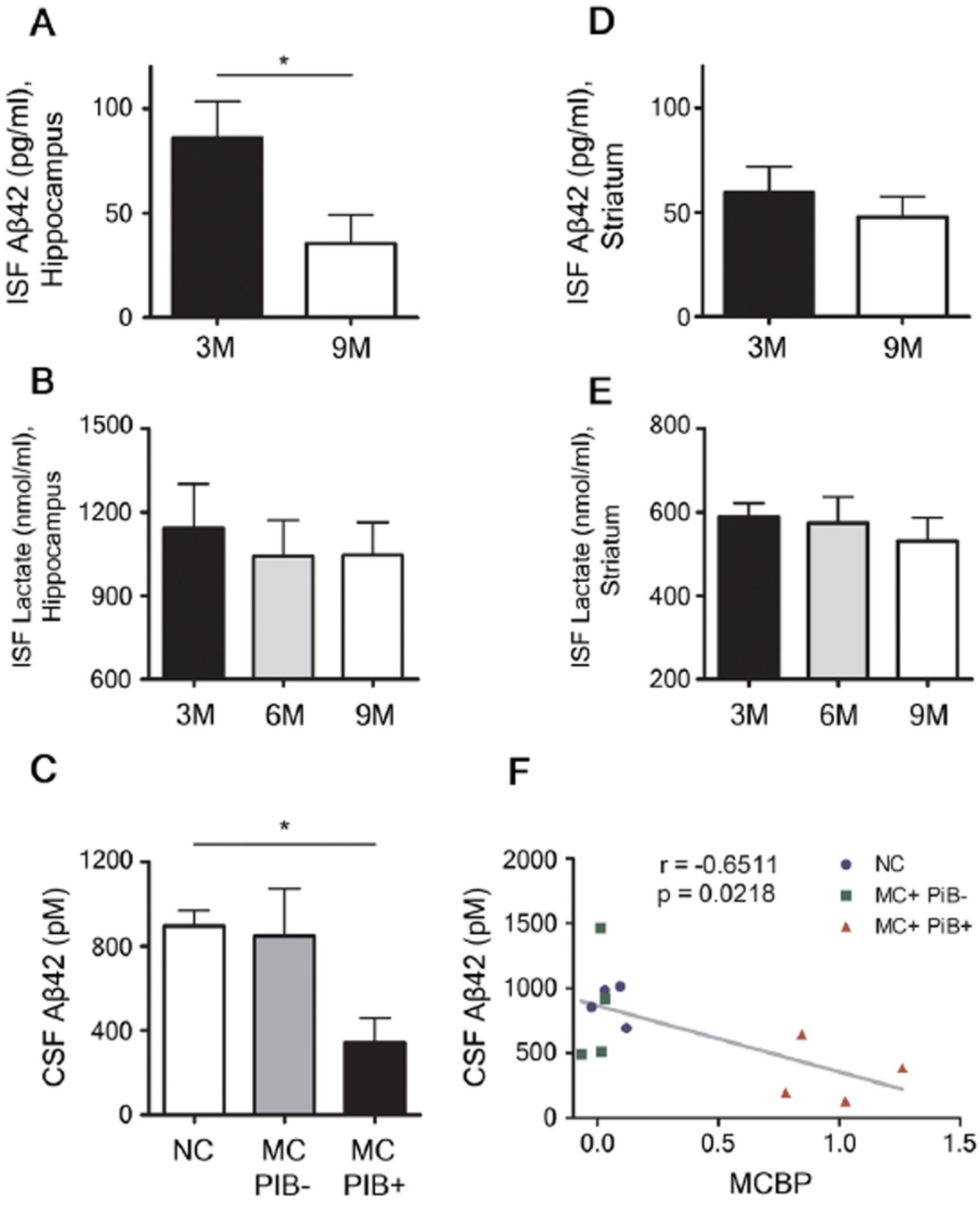

Figure 7.

Chronological changes of absolute concentrations of interstitial fluid (ISF) Aβ42 and lactate in the hippocampus and striatum of mice and association between CSF Aβ42 and amyloid plaque deposition in humans. **(A, D)** Absolute levels of ISF $A\beta_{x\text{-}42}$ in the hippocampus **(A)** and in the striatum **(D)** of 3 and 9 month old APPswe/PS1δE9 mice (n = 5–6 per group; Mann-Whitney Test). **(B, E)** Absolute levels of ISF lactate in the hippocampus **(B)** and in the striatum **(E)** of 3, 6, and 9 month old APPswe/PS1δE9 mice (n = 6 per group; one-way ANOVA, Tukey's*post hoc* test). **(C)** Comparison of absolute values of CSF Aβ42 in non-mutation carriers (NC), mutation carriers without amyloid plaque deposition (MC+PiB−),

mutation carriers with amyloid plaque deposition (MC+PiB+) (n = 4 per group; Kruskal-Wallis test). **(F)** Correlation between absolute levels of CSF Aβ42 and amount of amyloid plaque deposition measured by mean cortical PiB binding potential (MCBP) (n = 12 paired measurement; Pearson's correlation test). $*P < 0.05$; $**P < 0.01$. Values represent mean ± s.e.m.